

## VEGF autoregulates its proliferative and migratory ERK1/2 and p38 cascades by enhancing the expression of DUSP1 and DUSP5 phosphatases in endothelial cells

Sofia Bellou,<sup>1</sup> Mark A. Hink,<sup>2</sup> Eleni Bagli,<sup>1</sup> Ekaterini Panopoulou,<sup>3</sup> Philippe I. H. Bastiaens,<sup>2</sup> Carol Murphy,<sup>3</sup> and Theodore Fotsis<sup>1,3</sup>

<sup>1</sup>Laboratory of Biological Chemistry, Medical School, University of Ioannina, Ioannina, Greece; <sup>2</sup>Department of Systemic Cell Biology, Max-Planck-Institute for Molecular Physiology, Dortmund, Germany; and <sup>3</sup>Biomedical Research Institute/Foundation for Research & Technology-Hellas (BRI/FORTH), University Campus, Ioannina, Greece

Submitted 30 January 2009; accepted in final form 9 September 2009

**Bellou S, Hink MA, Bagli E, Panopoulou E, Bastiaens PI, Murphy C, Fotsis T.** VEGF autoregulates its proliferative and migratory ERK1/2 and p38 cascades by enhancing the expression of *DUSP1* and *DUSP5* phosphatases in endothelial cells. *Am J Physiol Cell Physiol* 297: C1477–C1489, 2009. First published September 9, 2009; doi:10.1152/ajpcell.00058.2009.—Vascular endothelial growth factor (VEGF) is a key angiogenic factor that regulates proliferation and migration of endothelial cells via phosphorylation of extracellular signal-regulated kinase-1/2 (ERK1/2) and p38, respectively. Here, we demonstrate that VEGF strongly induces the transcription of two dual-specificity phosphatase (DUSP) genes *DUSP1* and *DUSP5* in endothelial cells. Using fluorescence microscopy, fluorescence lifetime imaging (FLIM), and fluorescence cross-correlation spectroscopy (FCCS), we found that DUSP1/mitogen-activated protein kinases phosphatase-1 (MKP-1) was localized in both the nucleus and cytoplasm of endothelial cells, where it existed in complex with p38 (effective dissociation constant,  $K_D^{\text{eff}}$ , values of 294 and 197 nM, respectively), whereas DUSP5 was localized in the nucleus of endothelial cells in complex with ERK1/2 ( $K_D^{\text{eff}}$  345 nM). VEGF administration affected differentially the  $K_D^{\text{eff}}$  values of the DUSP1/p38 and DUSP5/ERK1/2 complexes. Gain-of-function and lack-of-function approaches revealed that DUSP1/MKP-1 dephosphorylates primarily VEGF-phosphorylated p38, thereby inhibiting endothelial cell migration, whereas DUSP5 dephosphorylates VEGF-phosphorylated ERK1/2 inhibiting proliferation of endothelial cells. Moreover, DUSP5 exhibited considerable nuclear anchoring activity on ERK1/2 in the nucleus, thereby diminishing ERK1/2 export to the cytoplasm decreasing its further availability for activation.

vascular endothelial growth factors; extracellular signal regulated kinase-1/2; p38; dual-specificity phosphatase 1/mitogen-activated protein kinase phosphatase-1; dual-specificity phosphatase-5

VASCULAR ENDOTHELIAL GROWTH FACTORS (VEGFs) are the most important regulators of vessel morphogenesis. Not only do they participate in the regulation of both vasculogenesis and angiogenesis, but they also are among the most important molecules involved in the pathogenesis of angiogenic diseases such as diabetic retinopathy and cancer (6). VEGFs are secreted dimeric glycoproteins of ~40 kDa, and in mammals the VEGF family consists of five members: VEGF-A, B, C, D and placental growth factor (PLGF) (6). Moreover, alternative splicing of several of the VEGF family members gives rise to isoforms with different biological activities. The VEGF ligands

bind in an overlapping pattern to three receptor tyrosine kinases known as VEGF receptor-1, -2, and -3 (VEGFR1–3), as well as to coreceptors such as heparan sulfate proteoglycans and neuropilins (22). VEGFR2 promotes migration, proliferation, and differentiation of endothelial cells (ECs) being critical for the regulation of angiogenic sprouting (1). Indeed, during sprouting, tip cells need to acquire an invasive and motile phenotype, whereas ECs in the stalk exhibit increased proliferation. In humans, upon VEGF-A binding, phosphorylation of VEGFR2 on Tyr-1175 leads to recruitment of PLC- $\gamma$ , which in turn, via activation of PKC, phosphorylates mitogen-activated protein kinase (MAPK)/extracellular signal-regulated kinase-1/2 (ERK1/2) leading to proliferation of ECs bypassing the classic Ras-Raf-MEK-MAPK pathway (30), although other reports implicate also the latter (21). Phosphorylation of Tyr-1214 of VEGFR2 activates stress-activated protein kinase-2/p38 (14) leading to VEGF-induced actin reorganization and migration of ECs via phosphorylation of heat-shock protein-27 (HSP27) (27) and LIM-kinase 1 (LIMK1) (13). Thus VEGF regulates EC proliferation and migration using MAPK-dependent pathways.

As MAPKs are activated by phosphorylation on threonine and tyrosine residues within a conserved signature sequence TxY by a MAPK kinase (MKK or MEK) (25), dual-specificity (Thr/Tyr) MAPK phosphatases (DUSPs/MKPs) are the largest group of phosphatases dedicated to the regulation of MAPK signaling in vertebrates (5). All DUSPs/MKPs contain a COOH-terminal catalytic HCX<sub>5</sub>R domain (31) and a NH<sub>2</sub>-terminal noncatalytic domain containing two regions of sequence similarity to the catalytic domain of the Cdc25 phosphatase (11). The NH<sub>2</sub>-terminal MKP domain also contains the kinase interaction motif (KIM), a cluster of basic amino acid residues followed by an LXL site or hydrophobic amino acids (31). The KIM domain exhibits high-affinity interactions with an acid-rich region termed the common docking domain (CD) in the COOH termini of all three MAPKs (31). Differences in the amino acid sequences of the CD and KIM domains fine-tune docking specificities between MAPKs and MKPs. In addition, MAPK binding to a MKP is often, but not always, accompanied by enzymatic activation of the COOH-terminal catalytic domain of the phosphatase thus ensuring specificity of action (23). Recent studies suggest essential roles for the DUSPs/MKPs in development, immune system function, metabolic homeostasis, and regulation of cellular stress responses (5).

Address for reprint requests and other correspondence: T. Fotsis, Biomedical Research Institute/Foundation for Research & Technology-Hellas (BRI/FORTH), Univ. Campus, 45110 Ioannina, Greece (e-mail: thfotsis@uoi.gr).

In the present study, using DNA microarrays and qRT-PCR, we demonstrate that, among other genes, *DUSP1* and *DUSP5* mRNAs are dramatically induced following VEGF administration in ECs peaking at 30 and 60 min, respectively. Using fluorescence microscopy, fluorescence lifetime imaging (FLIM), and fluorescence cross-correlation spectroscopy (FCCS), we have investigated the localization of DUSP1/MKP-1 and DUSP5 in ECs and characterized the interaction with their substrates p38 and ERK1/2. Finally, using gain-of-function and lack-of-function approaches, we have elucidated the functional role of DUSP1/MKP-1 and DUSP5 induction by VEGF in the regulation of VEGF-induced activation of ERK1/2 and p38 and the consequences on proliferation and migration of ECs, thereof.

## MATERIALS AND METHODS

**Cell culture.** Human umbilical vein ECs (HUVECs) were isolated and cultured as previously described (3, 7). HUVECs were pooled from at least five donors, and passage 2 to 5 was used for all experiments. For imaging experiments, cells were cultured at 37°C and 5% CO<sub>2</sub> in M199 imaging medium. Human kidney embryonal (293) cells were cultured in RPMI 1640 medium containing 10% FBS. Bovine brain capillary ECs were cultured in DMEM medium containing 10% newborn calf serum. EC growth supplement (ECGS) was isolated from a bovine brain as previously described (16) and was endotoxin-free (QCL-1000, Bio-Whittaker). All cells were routinely tested for mycoplasma. An antibody against von Willebrand factor, an endothelial marker, was used for ensuring cell homogeneity.

**Chemicals and antibodies.** MEK1 and p38 inhibitor, PD98059 and SB203580, respectively, were purchased from Sigma (Sigma, St. Louis, MO) and dissolved in DMSO. Phosphatase inhibitors okadaic acid and sodium orthovanadate were also from Sigma. Human VEGF<sub>165</sub> was purchased from ImmunoTools (Friesoythe, Germany). The polyclonal antibodies anti-DUSP1 and anti-p38 were from Santa Cruz Biotechnology (Santa Cruz, CA). The rabbit polyclonal anti-phospho-p38 (anti-P-p38), anti-ERK1/2, and anti-phospho-ERK1/2 (anti-P-ERK1/2) were obtained from Cell Signaling (Cell Signaling Technology, Beverly, MA). The anti-BrdU and anti-vinculin antibodies were from Sigma, and the mouse monoclonal anti-β-catenin was obtained from Signal Transduction Laboratories (BD Biosciences, Palo Alto, CA). The 9E10 (anti-Myc tag) monoclonal antibody was purified from the corresponding hybridoma using standard techniques. All secondary antibodies were purchased from Dianova (Hamburg, Germany).

**Constructs.** Myc-tagged DUSP1wt (DUSP1wt-myc) and Myc-tagged catalytically inactive DUSP1 (DUSP1/CS-myc) were kindly provided by Steve Keyse (Cancer Research UK, Biomedical Research Centre, Dundee, UK). Myc-tagged DUSP5wt (DUSP5wt-myc) and Myc-tagged catalytically inactive DUSP5 (DUSP5/CS-myc) were kindly provided by Jack Dixon (University of California, La Jolla, CA). The pRSET-B-mCherry vector was a gift from Roger Tsien (University of California, San Diego, CA) and was cloned into pcDNA3 vector by Panayiotis Kouklis (University of Ioannina, Ioannina, Greece). HA-ERK2 and HA-p38 were kindly provided by J. Silvio Gutkind (National Institutes of Health, Bethesda, MD). All expression vectors were from Invitrogen (Carlsbad, CA). The constructs DUSP1-eCFP, DUSP1-eGFP, eCFP-DUSP5, eGFP-DUSP5, p38-eYFP, p38-mCherry, eYFP-ERK2, ERK2-mCherry, eYFP-p38-eCFP, and eGFP-p38-mCherry were generated by PCR, sequenced by MWG (Ebersberg, Germany) and purified using Endo-Free kits from Qiagen (Qiagen) to avoid toxicity from LPS on HUVECs.

**Construction of recombinant adenoviruses.** DUSP1wt-myc and DUSP1/CS-myc (AdDUSP1wt or AdDUSP1/CS) were cloned into the *EcoRV* site of the expression vector pAD-CMV. DUSP5wt-myc (AdDUSP5wt) and DUSP5/CS-myc (AdDUSP5/CS) were cloned into

the *KpnI-XbaI* sites of pAD-CMV. Construction of recombinant adenoviruses followed as described ([www.coloncancer.org/adeasy.htm](http://www.coloncancer.org/adeasy.htm)). The adenovirus expressing β-galactosidase (AdLacZ) was kindly provided by A. Moustakas (Ludwig Institute for Cancer Research, Uppsala, Sweden). All vectors for the generation of adenoviruses were kindly provided by Bert Vogelstein (The Johns Hopkins Medical Institutions, Baltimore, MD).

**Transfection of HUVECs.** HUVECs were transfected 24 h after trypsinization with Metafectene-proreagent (Biontex, Biontex Laboratories, Martinsried/Planegg, Germany) at a DNA-to-lipid ratio 1:4. The complex was prepared in plain M199 medium and was incubated for 20 min at room temperature. Transfection complex was added to the cells in serum-reduced M199 medium (5% FBS) with no antibiotics, heparin, nor ECGS. Transfection medium was replaced with full HUVEC medium after 4 h.

**siRNA transfection.** For small interfering RNA (siRNA) experiments, siRNA for human DUSP1 (siDUSP1: 5'-GCACATTCGGACCAATATTT-3'), DUSP5 (siDUSP5: GGCCTTCGATTACATCAAG), and the control siRNA (Silencer Negative Control 5) were provided by Ambion. HUVECs were seeded at 50% confluence and siRNAs were transfected at a final concentration of 20 nM for 72 h with Lipofectamine RNAiMAX reagent (Invitrogen). Scrambled siRNA was included in each transfection as a control.

**Microarray analysis.** HUVECs, p6, pooled from 30 individuals (VEC Technology), was plated on 75-cm<sup>2</sup> dishes and cultured in M199 medium supplemented with 20% FCS, endothelial cell growth supplement (Sigma), heparin (Sigma), and penicillin-streptomycin. Cells were cultured until they reached 85% confluence and were serum starved for 6 h in M199 medium supplemented only with 5% FCS, heparin, and penicillin-streptomycin. Subsequently cells were induced with VEGF (30 ng/ml) for 3, 6, 12, 17, and 22 h. Total RNA was then isolated using RNeasy Kit (Qiagen). The concentration and the quality of the RNA were determined, and the samples were sent for microarray analysis to VIB facility (Belgium).

Microarray results were confirmed by quantitative reverse transcription-PCR (qRT-PCR) using The LightCycler 2.0 Instrument (Roche Diagnostics, Mannheim, Germany) and QuantiTect SYBR Green RT-PCR Kit (Qiagen). For qRT-PCR experiments, total RNA isolated at the time points indicated above was used along with RNA samples isolated after 0.5 and 1 h of VEGF induction.

**Indirect immunofluorescence.** HUVECs were grown on 11-mm coverslips at 3 × 10<sup>4</sup> cells per well and were treated as indicated in RESULTS, and indirect immunofluorescence followed as previously described (24). Samples were viewed with a Leica TCS-SP scanning laser confocal microscope equipped with an argon laser (for excitation at 488), solid-state 561 laser line, and helium-neon laser (for excitation at 633). Objectives used were Leica ×100 PL APO 1.4 NA and ×63 HCX PL APO 1.3 NA. Images were acquired using Leica software, and files were subsequently compiled in ImageJ and Adobe Photoshop.

**Nuclear and cytoplasmic extracts.** Nuclear and cytoplasmic extracts were prepared from control and VEGF-treated cells. Briefly, serum-starved HUVECs from 60-mm diameter dishes were induced with VEGF for various time points. The cells were then washed with PBS and 500 μl of ice-cold hypotonic buffer were added [20 mM Tris·HCl, pH 7.5, 10 mM NaCl, 1 mM DTT, 0.5% Nonidet-40, 0.2 mM EDTA, 5 mM MgCl<sub>2</sub>, 10% glycerol, 2 mM sodium vanadate, 50 nM okadaic acid, 20 mM β-glycerol phosphate, 50 mM sodium fluoride and protease inhibitors (Roche Diagnostics)]. The cells were allowed to swell on ice for 5 min, scraped, and centrifuged at 500 rpm for 5 min. The supernatant was collected as cytoplasmic fraction, and the pellet (nuclei) was resuspended in 500 μl hypertonic buffer (hypotonic buffer plus 500 mM NaCl). Equal volumes of these extracts were loaded on SDS-polyacrylamide gels for Western blotting with antibodies against P-ERK1/2 or ERK1/2. N-myc and Rab5 were used as nuclear and cytoplasmic markers, respectively.

**Cell proliferation.** HUVECs were seeded in 24-well plates onto 11-mm collagen-coated glass coverslips at  $3 \times 10^4$  cells per well, and after overnight incubation the HUVECs were infected with adenoviruses AdLacZ, AdDUSP1wt, AdDUSP5wt, or the catalytically inactive mutants of either AdDUSP1/CS or AdDUSP5/CS at a multiplicity of infection (MOI) of 200. After 24 h, cells were placed into reduced HUVEC-medium containing 5% FBS lacking ECGS for 16 h. The cells were then stimulated with 50 ng/ml VEGF and incubated for 24 h. For the final 6 h, cells were treated with 100  $\mu$ M bromodeoxyuridine (BrdU, Sigma). Cells were then fixed and processed for indirect immunofluorescence as previously described (24).

**Cell migration assay.** Twenty four hours postinfection (AdLacZ and AdDUSP1wt at MOI 200 or AdLacZ and AdDUSP5wt at MOI 300), confluent HUVEC monolayers were wounded with a sterile plastic pipette tip, cultured in M199 medium supplemented with 5% FCS, and induced with VEGF (10 ng/ml). Cells were placed in a 37°C, 5% CO<sub>2</sub> chamber and monitored using a Leica DM IBRE microscope equipped with a HRD060-NIK CCD-camera (Diagnostic Instruments, Sterling Heights, MI) and Metamorph software. Frames were taken every 10 min for 16 h. Results were expressed as number of cells per centimeter of wound.

**Fluorescence cross-correlation spectroscopy.** FCCS was performed using a Zeiss LSM510-Meta-Confocor 3 (Carl Zeiss Jena) following the procedure as described previously (17). A water immersion C-Apochromat  $\times 40$  objective lens (NA 1.2) was used. To establish FCCS, a positive control expressing a fusion of eGFP-p38-mCherry was used. Average cross-correlation amplitude corresponding to 67% complex was obtained. The failure to detect 100% cross-correlation arose from imperfect overlap of the two confocal detection volumes at the respective excitation wavelengths. Where VEGF induction is indicated, cells were serum-starved for 2 h in plain M199 before growth factor stimulation. The raw data files were correlated and analyzed using the FCS Dataprocessor 1.5 software (SSTC, Belarusia).

**Fluorescence lifetime imaging in living cells.** FLIM measurements of enhanced cyan fluorescent protein (eCFP) were performed in living HUVECs as described previously (17). Briefly, eCFP was excited with a 440-nm diode (Sepia II, Picoquant, Germany). Emission light passed a 440/530 dichroic mirror and was guided via a multimode fiber into the detection box containing a HQ480DF40 emission filter and a single avalanche photon detector (MPD, Italy). A water immersion  $\times 60$  UPlanSApo objective lens (numerical aperture 1.2) was used. Images of  $256 \times 256$  pixels were acquired during 4 min corresponding to approximately 1 million detected photons. Images of the donor fluorescence were processed using the SymPhoTime software package (v4.2, Picoquant). The images were analyzed on a pixel-to-pixel basis using a two-exponential fitting model including background. Both fluorescence lifetimes, corresponding to the populations of non- and interacting eCFP proteins, were retrieved from analysis of the summed photon count histograms of control and sample and fixed during analysis.

## RESULTS

**VEGF enhances transcription of DUSP1 and DUSP5 genes in ECs.** To identify genes that are regulated by VEGF in ECs, we have carried out DNA microarray analysis on mRNA collected from HUVECs at several time points post-VEGF induction. From  $\sim 22,000$  genes examined, VEGF increased the expression of 116 genes, whereas it decreased the expression of 30 genes. *DUSP1* and *DUSP5* were among the genes that exhibited a statistically significant increase in their expression at several time points post-VEGF induction. Though most of the other DUSP genes (*DUSP 2, 4, 7, 8, 9, 10, and 16*) were included in the DNA chip, none of them exhibited statistically significant regulation by VEGF. Validation by qRT-PCR re-

vealed that the mRNA levels of *DUSP1* and *DUSP5* were induced almost 20- and 10-fold at 30 and 60 min post-VEGF induction, respectively (Fig. 1A), compatible with the notion that these *DUSPs* are immediate early genes (8). qRT-PCR also revealed that VEGF did not exhibit any regulatory effects on the expression of the *DUSP6* gene, the only DUSP missing from the DNA chip, or the *DUSP4* and *13* genes that were also slightly upregulated at 3 h in the microarray analysis (Fig. 1B). These results suggest that VEGF increases the expression of *DUSP1* and *DUSP5* genes, at 30 and 60 min, respectively, in ECs.

VEGF increased significantly the level of DUSP1/MKP-1 protein after 30 min of induction in HUVECs (Supplemental Fig. 1A). The increase in DUSP1/MKP-1 protein was, however, much weaker compared with the strong (20-fold) VEGF-induced upregulation of the *DUSP1* gene. Because binding of P-ERK1/2 to DUSP1/MKP-1 causes proteolytic degradation of the phosphatase (15), we wondered whether VEGF-induced P-ERK1/2 and P-p38 might exert such regulation. Indeed, in cycloheximide-treated HUVECs, VEGF reduced considerably the half-lifetime of DUSP1/MKP-1 from 4.5 to 3 h (supplemental Fig. 1B). Unfortunately, because of the lack of a reliable antibody against DUSP5, a similar experiment with endogenous DUSP5 could not be performed.

*DUSP1 is localized in the nucleus, cytoplasm, and on the cell membrane of ECs.* Indirect immunofluorescence revealed that endogenous DUSP1/MKP-1 was present in both the nucleus and cytoplasm of HUVECs (Fig. 1C), although DUSP1/MKP-1 is considered to be an inducible nuclear protein (10). Furthermore, in 50% of the cells, DUSP1/MKP-1 was found on the plasma membrane colocalizing with  $\beta$ -catenin (used as marker of the plasma membrane) (Fig. 1C, bar graph). Indeed, DUSP1/MKP-1 was present in both the nuclear and cytoplasmic fractions of HUVECs (Fig. 1D). In addition, overexpressed enhanced green fluorescent protein (eGFP)-labeled DUSP1/MKP-1 was localized in both the nucleus and cytoplasm of ECs (Fig. 1E) confirming the results with the endogenous protein (Fig. 1C), whereas eGFP-DUSP5 exhibited strictly nuclear localization even at high expression levels (Fig. 1E). In agreement, siRNA knockdown of *DUSP1* (supplemental Fig. 2) leads to decreased cytoplasmic and nuclear staining of the phosphatase (Fig. 1F). Therefore, we conclude that DUSP1/MKP-1 is not only localized in the nucleus but is also present in the cytoplasm and on the plasma membrane of ECs.

*DUSP1 and DUSP5 interact mainly with p38 and ERK2, respectively, and this interaction is differentially affected by VEGF treatment in the nucleus of HUVECs.* Determining the substrate specificity of DUSPs has been under extensive investigation during the last years. However, this effort has been proven challenging since regulation of MAPK by DUSPs may be cell type and stimulus specific (8). In addition, results from in vitro assays do not always reflect physiological roles in vivo. To reach a better understanding of these enzyme-substrate interactions, we estimated the strength of DUSP1-p38 and DUSP5-p38 interactions using FCCS in living HUVECs (2). Indeed, with the use of DUSP1-eGFP and p38-mCherry constructs, the effective dissociation constant ( $K_D^{\text{eff}}$ ), as defined previously (17), of the DUSP1-p38 interaction was estimated in the cytoplasm of HUVECs (Fig. 2A), being essentially identical in full serum ( $291 \pm 62$  nM) or 2 h of serum starvation ( $294 \pm 23$  nM). The corresponding values for the

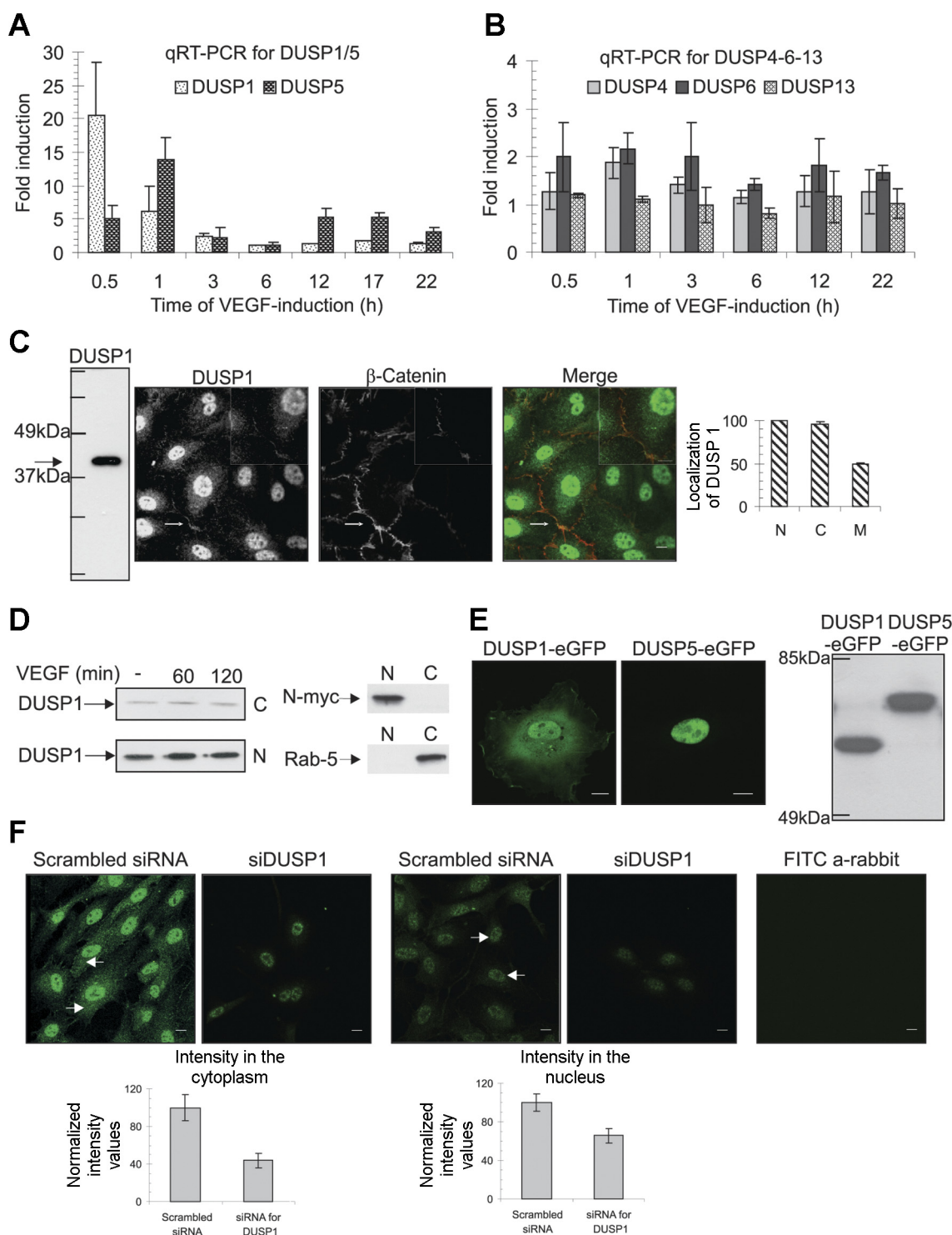


Fig. 1. Effect of vascular endothelial growth factor (VEGF) on dual-specificity phosphorylation (DUSP) *DUSP1* and *DUSP5* genes and DUSP1/mitogen-activated protein kinase phosphorylation-1 (MKP-1) localization in endothelial cells. *A* and *B*: total RNA was isolated after the indicated time points of VEGF-induction of human umbilical vein endothelial cells (HUVECs) and expression of *DUSP1-5* (*A*) and *DUSP3-6-14* (*B*) was examined by qRT-PCR. Numbers present means  $\pm$  SD of four independent experiments. *C*: For indirect immunofluorescence, anti-DUSP1/MKP-1 and anti- $\beta$ -catenin were used as primary antibodies against endogenous proteins and FITC anti-rabbit and TRITC anti-mouse IgG as secondary antibodies. The average number of cells in which endogenous DUSP1/MKP-1 was nuclear (N), cytoplasmic (C), and on cell membrane (M)  $\pm$  SD of three independent experiments is presented. Bar, 10  $\mu$ m. Arrows indicate plasma membrane localization of DUSP1. *D*: serum-starved HUVECs were stimulated with VEGF (50 ng/ml) for various time points. Cells were then subjected to cell fractionation. N-myc and Rab5 were used as nuclear or cytoplasmic markers, respectively. A representative experiment from four independent experiments is shown. *E*: HUVECs were transfected with either DUSP1-GFP or DUSP5-GFP. After 24 h, cells were fixed, mounted, and visualized by fluorescence microscopy. Lysates from transfected cells were used for immunoblotting with anti-green fluorescent protein (GFP) as primary antibody. Bar, 10  $\mu$ m. *F*: HUVECs transfected with scrambled small interfering RNA (siRNA) or siDUSP1 for 72 h were fixed, mounted, and visualized by fluorescence microscopy. Quantitation of intensity in the cytoplasm (*left*) and in the nucleus (*right*) of more than 100 cells was carried out using ImageJ on the raw data. Graphs present means  $\pm$  SD of intensity. The experiment shown is a representative one from three independent experiments.

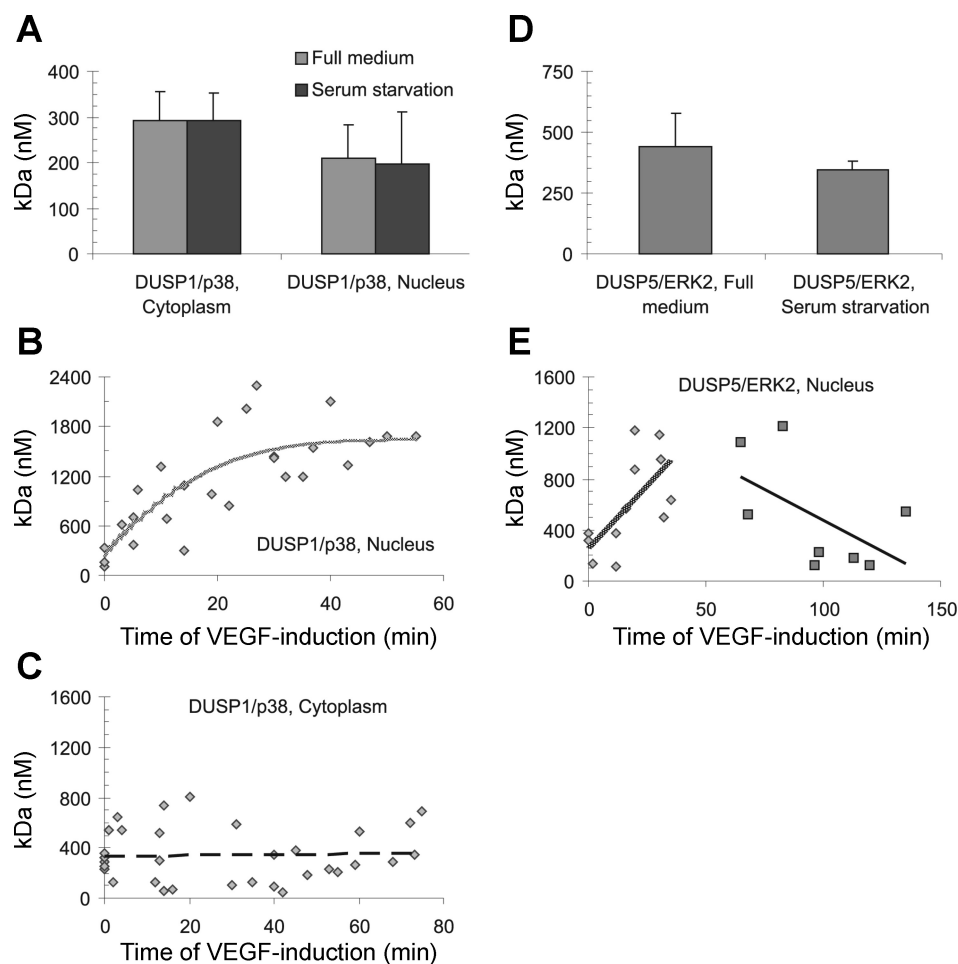


Fig. 2. VEGF affects differently the DUSP1/p38 and DUSP5/ERK1/2 interactions in the nucleus of endothelial cells. *A*: HUVECs were cultured in collagen-coated chambers until they reached 50% confluence before transfection with DUSP1-eGFP and mCherry vector or DUSP1-eGFP and p38-mCherry. Fluorescence cross-correlation spectroscopy (FCCS) measurements were taken in 20–50 cells either in full medium or after 2 h serum starvation. *B* and *C*: FCCS measurements were taken after VEGF induction (50 ng/ml) and the effective dissociation constant ( $K_D^{\text{eff}}$ ) values of the DUSP1/p38 interaction at various time points were measured in the nucleus (*B*) and in cytoplasm (*C*) of HUVECs. *D*: HUVECs were transfected with DUSP5-eGFP and mCherry vector or DUSP5-eGFP and ERK2-mCherry. FCCS measurements were taken in 20–50 cells in either full medium or after 2 h serum starvation. *E*: FCCS measurements were taken after VEGF induction (50 ng/ml) and the  $K_D^{\text{eff}}$  values of the DUSP5/ERK2 interaction at various time points were measured in the nucleus of HUVECs.

nuclear DUSP1-p38 interaction were  $209 \pm 27$  in full medium and  $197 \pm 66$  after 2 h of serum starvation (Fig. 2A). The  $K_D^{\text{eff}}$  of the DUSP5-eGFP-p38mCherry interaction was  $1,314 \pm 149$  nM in full medium suggesting that DUSP5 and p38 interact very weakly, if not at all. Interestingly, VEGF treatment of HUVECs considerably decreased the affinity of DUSP1-p38 interaction (increased the  $K_D^{\text{eff}}$  value from  $197 \pm 66$  to  $1,505 \pm 256$  nM) in the nucleus (Fig. 2B and supplemental Fig. 3A), whereas it had no effect on the DUSP1-p38 interaction in the cytoplasm (Fig. 2C and supplemental Fig. 3B).

Similar evaluation, using ERK2-mCherry, DUSP5-eGFP, and DUSP1-eGFP constructs, revealed that the  $K_D^{\text{eff}}$  of DUSP5-ERK2 interaction in the nucleus of HUVECs was  $441 \pm 135$  and  $345 \pm 37$  nM in full medium or 2 h after serum starvation, respectively (Fig. 2D), whereas that of DUSP1-ERK2 in full medium was weaker ( $603 \pm 141$  nM). VEGF induction affected the affinity of DUSP5-ERK2 interaction in the nucleus of HUVECs in a bimodal manner. It initially increased the  $K_D^{\text{eff}}$  to  $816 \pm 310$  nM at 35 min after VEGF induction, thereafter decreasing it to  $150 \pm 38$  nM at 130 min after VEGF induction (Fig. 2E and supplemental Fig. 3C).

Next, we have used FLIM in living ECs to confirm the above findings. In these experiments, if the eCFP-tagged phosphatase interacted with the relevant enhanced yellow fluorescent protein (eYFP)-tagged MAPK leading to fluorescence resonance energy transfer (FRET), this would result in a decrease in the

donor fluorescence lifetime (34). Indeed, the fluorescence lifetime of eCFP-DUSP1 was decreased statistically significantly from  $2.53 \pm 0.04$  ns (in presence of the eYFP vector) to  $2.28 \pm 0.07$  ns, when HUVECs were transfected with p38-eYFP (Fig. 3B); the construct eCFP-p38-eYFP was used as a positive control (Fig. 3A). In agreement with the nuclear and cytoplasmic localization of DUSP1, the interaction with p38 occurred in both compartments. Similarly, the fluorescence lifetime of DUSP5-eCFP was decreased from  $2.53 \pm 0.02$  to  $2.22 \pm 0.07$  ns in the presence of ERK2-eCFP and it was confined only to the nucleus (Fig. 3C).

When taken together these data suggest that, in living HUVECs, DUSP1 interacts strongly with p38, the interaction with ERK2 being weaker. DUSP5 interacts strongly only with ERK2. VEGF administration affects the DUSP1-p38 and DUSP5-ERK2 interactions differently in the nucleus of HUVECs, strongly suggesting that these complexes have a different fate after VEGF induction. The bimodal change in the  $K_D^{\text{eff}}$  of the DUSP5-ERK2 complex is compatible with the anchoring effect of DUSP5 on ERK1/2 in the nucleus of HUVECs (see below).

*DUSP1 regulates VEGF-induced phosphorylation of p38 in ECs.* VEGF activation of p38 is one of the main pathways that stimulate EC migration, a key partial step of angiogenic sprouting (13, 14, 27). Indeed, in HUVECs, VEGF-induced p38 phosphorylation peaked at 5 min, fully returning to background levels within 40 min (Fig. 4, A and D), whereas phosphoryla-

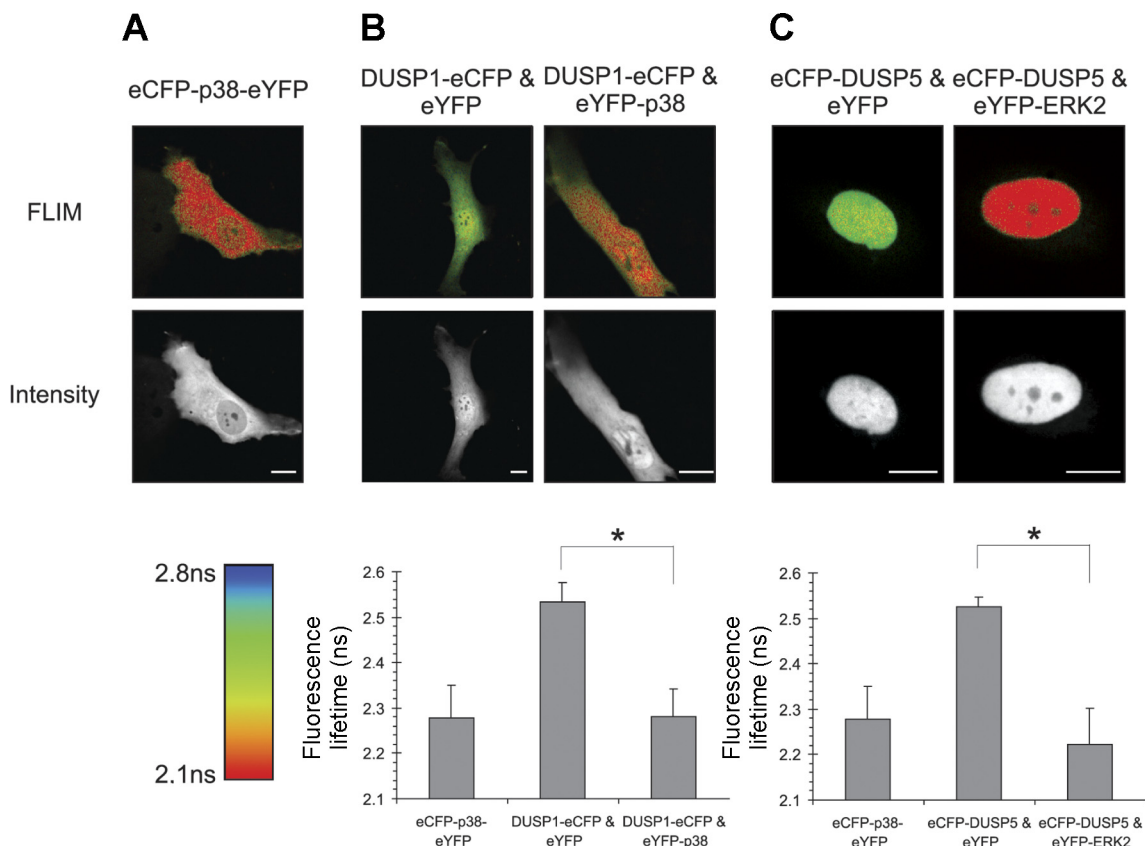


Fig. 3. DUSP1 and DUSP5 interact with p38 and ERK2, respectively, in living endothelial cells. HUVECs were cultured in collagen-coated chambers until they reached 50% confluence. Then they were transfected with enhanced cyan fluorescent protein (eCFP)-p38-enhanced yellow fluorescent protein (eYFP) fusion protein (A) or DUSP1-eCFP and eYFP vector or DUSP1-eCFP and p38-eYFP (B), or DUSP5-eCFP and eYFP vector or DUSP5-eCFP and ERK2-eYFP (C). After 24 h, fluorescence lifetime imaging (FLIM) experiments were performed according to MATERIALS AND METHODS. The eCFP intensity images are shown, the pseudo-colored FLIM and the plots displaying the fluorescence lifetime distribution averaged over several cells. Bar, 10  $\mu$ m. Values present means  $\pm$  SD of fluorescence lifetime. The experiment shown is a representative one from three independent experiments. \* $P < 0.0001$ .

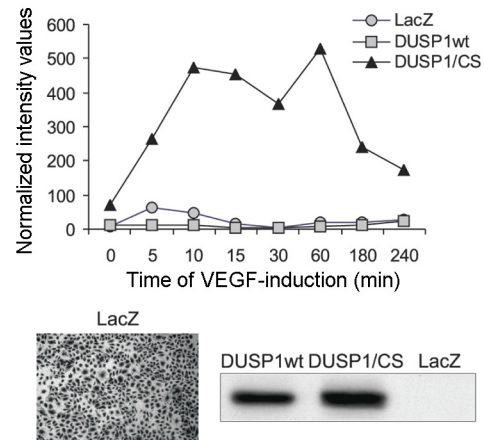
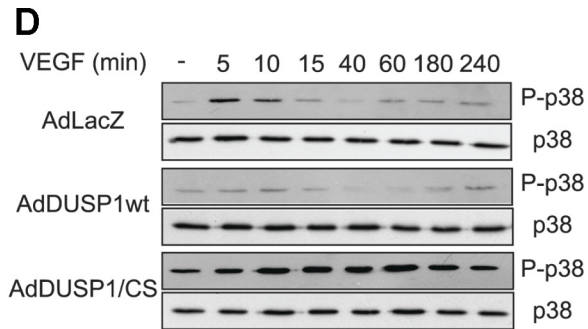
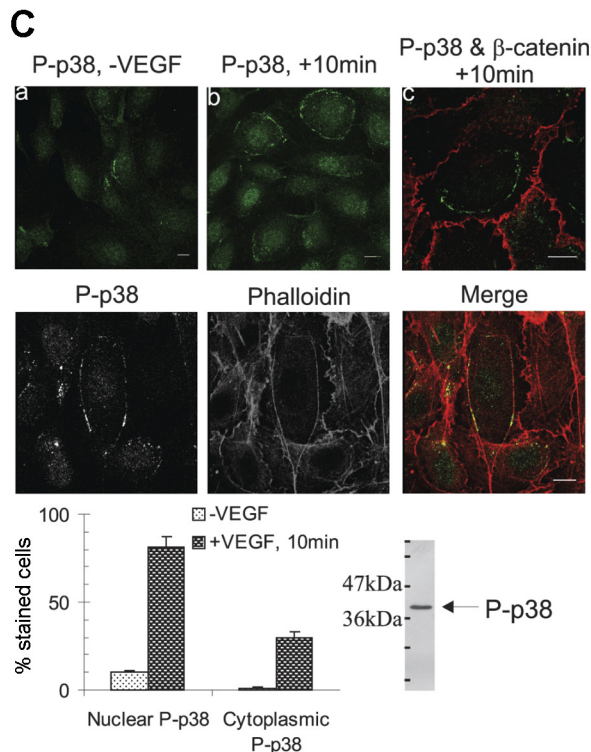
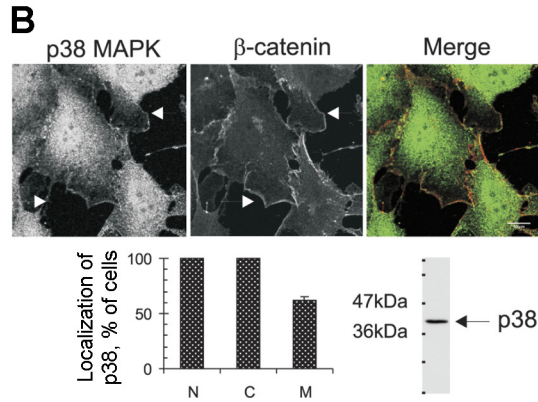
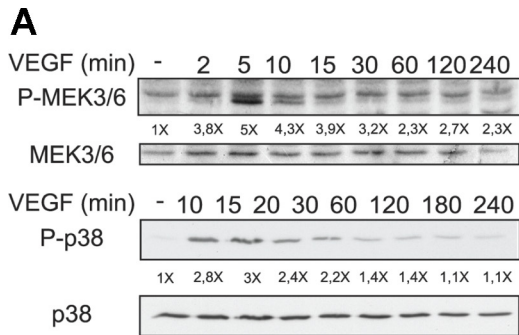
tion of MEK3/6 also peaked at 5 min but retained a higher than background level of phosphorylation throughout the experiment (240 min) (Fig. 4A). In nonstimulated cells, p38 was found in the nucleus, cytoplasm, and plasma membrane (colocalization with  $\beta$ -catenin) (Fig. 4B). VEGF induction increased the nuclear localization of phosphorylated p38 (P-p38) from 10% to 70%, (Fig. 4C,a,b and bar graph), however, in 30% of the cells (Fig. 4C, bar graph) P-p38 exhibited a membrane-like localization (Fig. 4C,b), which upon costaining with  $\beta$ -catenin was clearly within the cytoplasm (Fig. 4C,c). Further characterization revealed that P-p38 colocalized with labeled phalloidin (Fig. 4C, bottom) suggesting localization on the actin cytoskeleton, where it could influence actin reorganization and migration of ECs (13).

Next, we investigated whether DUSP1/MKP-1 could influence the kinetics of VEGF-induced phosphorylation of p38. Indeed, overexpression of DUSP1/MKP-1 led to complete inhibition of VEGF-induced phosphorylation of p38, whereas overexpression of a dominant negative (catalytically inactive) form of DUSP1 (DUSP1/CS) resulted in a dramatic increase of both the duration and magnitude of VEGF-induced phosphorylation of p38 (Fig. 4D). The wild-type and dominant-negative forms of DUSP5 had no effect on VEGF-induced activation of p38 (data not shown). The result is compatible with our FCCS data and the known selectivity of DUSP5 toward ERK1/2 (19) suggesting that DUSP1/MKP-1 may be the predominant DUSP that feedbacks on VEGF-induced phosphorylation of p38.

Fig. 4. MKP-1/DUSP1 regulates VEGF-induced phosphorylation of p38 in endothelial cells. A: HUVECs were serum starved in M199 medium for 2 h. VEGF (50 ng/ml) was added and cell lysates were used for immunoblotting. Representative experiment from four independent experiments is shown. Values represent the fold induction at each time point compared with the noninduced sample. B: HUVECs were cultured in full medium. Indirect immunofluorescence was performed with primary antibodies against endogenous p38 and  $\beta$ -catenin. Bottom: average number of cells in which endogenous p38 was nuclear (N), cytoplasmic (C), and cell membrane associated (M)  $\pm$  SD of three independent experiments. HUVEC lysate was used for Western assay to ensure antibody specificity. Bar, 10  $\mu$ m. C: serum-starved HUVECs were stimulated with VEGF (50 ng/ml) for 10 min. Indirect immunofluorescence was carried out using primary antibodies against endogenous P-p38 and  $\beta$ -catenin (top) or staining with labeled-phalloidin (bottom). Graph presents average number of cells in which endogenous P-p38 was nuclear or cytoplasmic before or after VEGF-induction  $\pm$  SD of three independent experiments. Lysates from stimulated HUVECs were used for ensuring antibody specificity. See RESULTS for details about a-c. Bar, 10  $\mu$ m. D: HUVECs were infected with AdLacZ, AdDUSP1wt, or AdDUSP1/CS for 24 h. They were then serum starved for 2 h and induced with VEGF (50 ng/ml) for various time points. Immunoblotting was performed with antibodies against endogenous P-p38 or p38. Graph shows normalized intensities in arbitrary units. Bottom: infection efficiency with AdLacZ adenovirus and expression levels of AdDUSP1wt and AdDUSP1/CS. One representative experiment, from three performed, is presented.

*DUSP5 and DUSP1 regulate VEGF-induced phosphorylation of ERK1/2 in ECs.* VEGF stimulates EC proliferation via phosphorylation of ERK1/2 (28, 30). In HUVECs, VEGF caused phosphorylation of ERK1/2 peaking at 10 min and returning to background levels within 40 min (Fig. 5A). On the other hand, VEGF-induced phosphorylation of MEK1/2, the

upstream activator of ERK1/2, reached a maximum at 5 min, retaining phosphorylation levels above background for up to 4 h (Fig. 5A). Interestingly, upon VEGF activation, only a small proportion of P-ERK1/2 was found in the nucleus, the majority being localized at focal adhesions costaining with vinculin (Fig. 5B). Use of PD98059 (an inhibitor of MEK1)



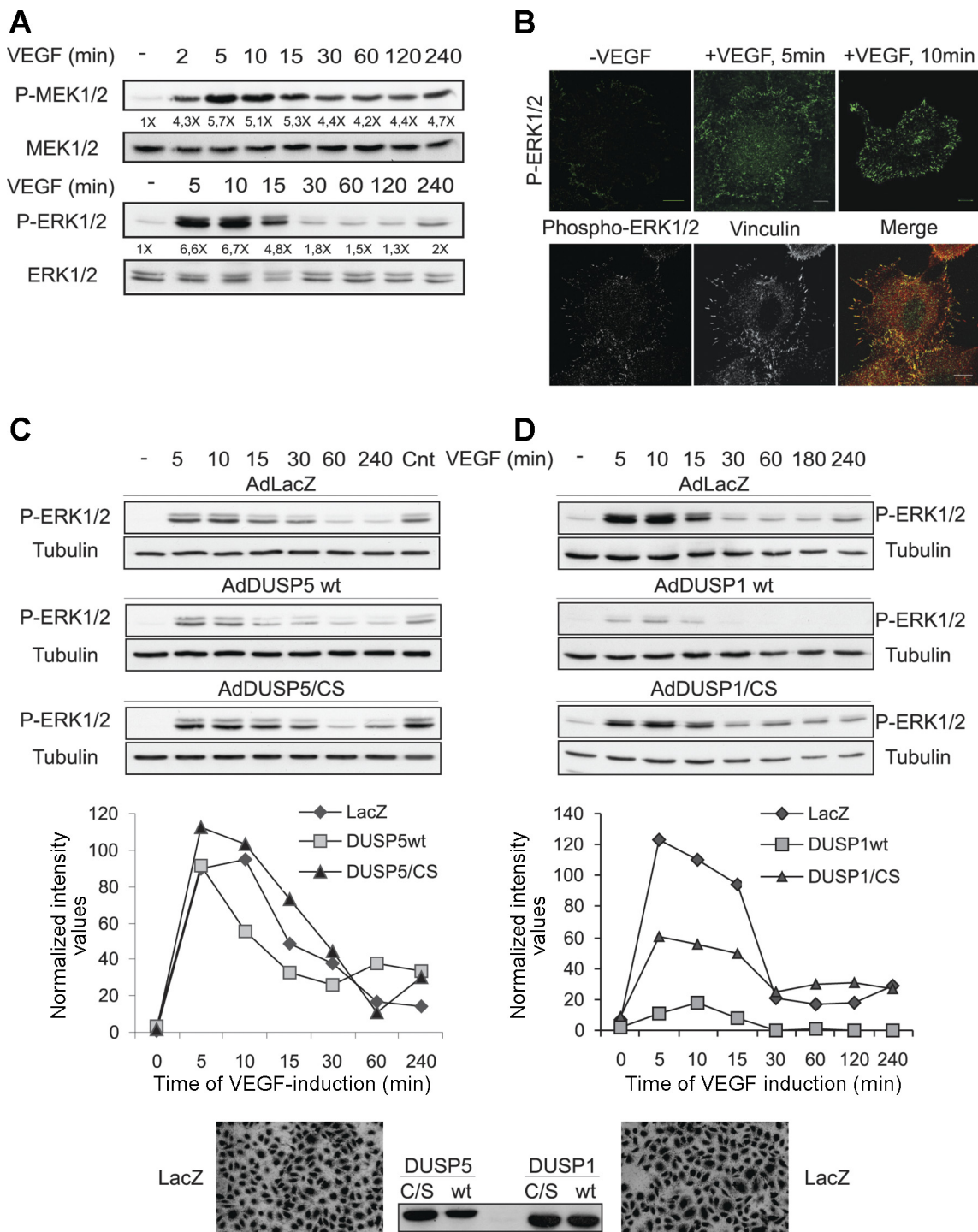


Fig. 5. Kinetics and localization of extracellular signal-regulated kinase 1/2 (ERK1/2) phosphorylation upon VEGF induction in HUVECs. *A*: serum-starved HUVECs were stimulated with VEGF (50 ng/ml) for various time points. Immunoblotting was carried out with antibodies against endogenous P-MEK1/2, MEK1/2, P-ERK1/2, and ERK1/2. Values represent the fold induction at each time point compared with the noninduced sample. Representative experiment from three independent experiments is shown. *B*: serum-starved HUVECs were stimulated with VEGF (50 ng/ml) for 5 or 10 min. Indirect immunofluorescence followed using antibodies against endogenous P-ERK1/2 and vinculin. Bar, 10  $\mu$ m. *C*: HUVECs were infected with AdLacZ or AdDUSP5wt or AdDUSP5/CS for 24 h. Serum-starved cells were then induced with VEGF (50 ng/ml) for various time points. Immunoblotting followed using antibodies against endogenous P-ERK1/2 and tubulin. For intensity normalization between different gels, we used a common sample as a control (Cnt). *Bottom*: infection efficiency with AdLacZ and expression levels of DUSP5wt and DUSP5/CS. The experiment shown is a representative one from five independent experiments. *D*: HUVECs were infected with AdLacZ, AdDUSP1 wt, or AdDUSP1/CS for 24 h. Serum-starved cells were induced with VEGF (50 ng/ml) for various time points. Immunoblotting followed using antibodies against endogenous P-ERK1/2 and tubulin. *Bottom*: infection efficiency with AdLacZ and expression levels of AdDUSP1wt and AdDUSP1/CS. The experiment shown is a representative one from three independent experiments.

effectively reduced VEGF-induced P-ERK1/2 activation and staining, whereas employment of phosphatase inhibitors (sodium orthovanadate and okadaic acid) had exactly the opposite effect (supplemental Fig. 4, A and B), verifying the specificity of the antibody against P-ERK1/2. Cell fractionation fully confirmed that VEGF did not exhibit any significant nuclear localization of P-ERK1/2 (data not shown). Thus we conclude that VEGF-induced P-ERK1/2 is found predominantly at focal adhesions exhibiting minor nuclear staining.

Sustained activation of MEK1/2 accompanied by transient phosphorylation of ERK1/2 suggested that dephosphorylation of the latter may be a key factor that restricts the magnitude and duration of VEGF-induced ERK1/2 activation. Overexpression of DUSP5 led to a slight decrease in the duration of ERK1/2 phosphorylation without affecting its intensity (Fig. 5C), whereas overexpression of DUSP1 resulted in efficient dephosphorylation of P-ERK1/2 (Fig. 5D). The result is compatible with DUSP5 being exclusively localized in the nucleus (Fig. 1E), whereas DUSP1 is localized also in the cytoplasm being able to dephosphorylate the bulk of VEGF-induced P-ERK1/2 at focal adhesions (Fig. 5B). However, the strong effect of DUSP1 on P-ERK1/2 is probably the result of overexpression, and it is unlikely that at endogenous levels DUSP1 will have such an impact. Indeed, overexpressing the dominant-negative mutant DUSP1/CS (Fig. 5D) or siRNA silencing of DUSP1 (supplemental Fig. 5A) did not lead to increased P-ERK1/2, the latter being actually decreased indicating that DUSP1 is not the

only phosphatase responsible for dephosphorylation of VEGF-induced P-ERK1/2. On the other hand, overexpressing the dominant-negative mutant DUSP5/CS (Fig. 5C) or siRNA silencing of DUSP5 (supplemental Fig. 5B) did increase the intensity of VEGF-induced phosphorylation of ERK1/2 albeit only at early time points. These results indicate that DUSP5 contributes to the overall dephosphorylation of VEGF-induced P-ERK1/2.

*DUSP5 dephosphorylates and anchors ERK1/2 in the nucleus of ECs.* How could the nuclear DUSP5 contribute in P-ERK1/2 dephosphorylation, when the latter exhibited minimal nuclear localization being detected predominantly on focal adhesions following VEGF induction? One explanation is that nuclear DUSP5 concentrations (pre- and post-VEGF induction), as well as other DUSPs, efficiently dephosphorylate P-ERK1/2 that is translocated to the nucleus, thereby allowing only a minimal increase of VEGF-induced nuclear P-ERK1/2 levels (Fig. 5B). Indeed, P-ERK1/2 could be detected in the nucleus of DUSP5/CS-expressing cells (Fig. 6A, j–l), because the catalytically inactive DUSP5/CS was unable to dephosphorylate it. Actually, more than 95% of the HUVECs infected with the adenovirus expressing DUSP5/CS exhibited strong nuclear staining of P-ERK1/2 after VEGF induction compared with only 9–10% of the noninduced cells (Fig. 6n). Moreover, DUSP5 has been reported to function as a nuclear anchor for ERK2 in mammalian cells (19) sequestering ERK1/2 in the nucleus, thereby decreasing recycling of ERK1/2 to the cyto-

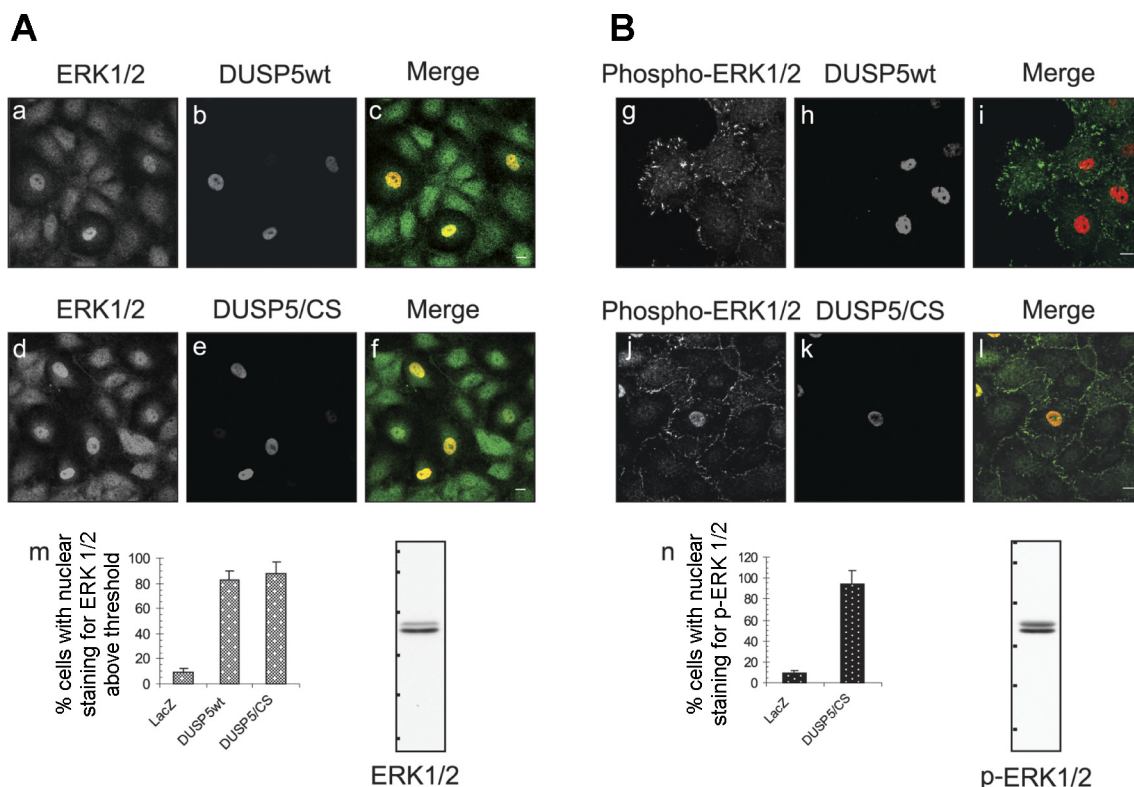


Fig. 6. Effect of DUSP5 on VEGF-induced phosphorylation and localization of ERK1/2. HUVECs were infected with AdLacZ, AdDUSP5wt, or AdDUSP5/CS for 24 h. Serum-starved cells were then induced by VEGF (50 ng/ml) for 10 min. Subsequently, indirect immunofluorescence was carried out using either anti-P-ERK1/2 or anti-ERK1/2, or anti-myc as primary antibodies. See RESULTS for details about a–l. *Bottom left*: average number of the cells with nuclear staining of ERK1/2 above threshold  $\pm$  SD of three independent experiments. *Bottom right*: mean percentage of cells with nuclear staining of P-ERK1/2 above threshold  $\pm$  SD of three independent experiments. Immunoblotting using HUVEC-lysates and antibodies against P-ERK1/2 and ERK1/2 ensured antibody specificity. Bar, 10  $\mu$ m.

plasm for further activation and in this way functioning as an efficient mechanism for signal termination (33) (see also DISCUSSION). Indeed, we have observed that infection of HUVECs with adenoviruses expressing either DUSP5 or DUSP5/CS resulted in a dramatic increase in the intensity of nuclear ERK1/2 staining in more than 80% of the infected cells (Fig. 6, *a-f, m*). Therefore, DUSP5-dependent ERK1/2 nuclear anchoring could have contributed to the considerable increase of VEGF-induced P-ERK1/2 nuclear staining following overexpression of DUSP5/CS (Fig. 6, *j-l, n*), possibly decreasing the cytoplasmic pool of ERK1/2 available for activation. Taken together, these results suggest that DUSP5 appears to participate in the rapid dephosphorylation of P-ERK1/2 imported to the nucleus exhibiting also a strong nuclear anchoring activity on ERK1/2.

*Overexpression of DUSP1 and DUSP5 inhibits VEGF-induced migration and proliferation of ECs.* VEGF-induced activation of p38 and ERK1/2s has been linked to the regulation of migration and proliferation of ECs, respectively (22). Indeed, VEGF induced, in a statistically significant manner, migration of HUVECs both using the wounding (Fig. 7A, *top*) and transwell (data not shown) assays, whereas SB203580, a

specific inhibitor of p38, totally abolished VEGF-induced migration of ECs in the wounding assay (data not shown). Infection of HUVECs with the adenovirus expressing DUSP1/MKP-1 resulted in a dramatic inhibition of basal and VEGF-induced EC migration compared with control cells (Fig. 7A). The result is compatible with the decrease in VEGF-induced p38 activation, when DUSP1/MKP-1 was overexpressed in ECs (Fig. 4D). On the contrary, overexpression of DUSP5 did not have any appreciable effect on VEGF-induced migration of HUVECs in wound healing assays (Fig. 7A). Thus DUSP1/MKP-1 is critical for dephosphorylating VEGF-induced P-p38 levels, thereby controlling VEGF-induced migration of ECs.

Next, we investigated the effect of DUSP1/MKP-1 and DUSP5 overexpression on VEGF-induced EC proliferation. As VEGF induces EC proliferation via activation of the ERK1/2s (30), employment of PD98059, an inhibitor of MEK1, dramatically decreased VEGF-induced BrdU incorporation in HUVECs (data not shown). Infection of adenoviruses expressing either DUSP1 or DUSP5 abolished almost completely VEGF-induced BrdU incorporation in HUVECs compared with the effect of the control adenovirus infection (Fig. 7, *B, left and middle*). However, overexpression of DUSP5/CS resulted in

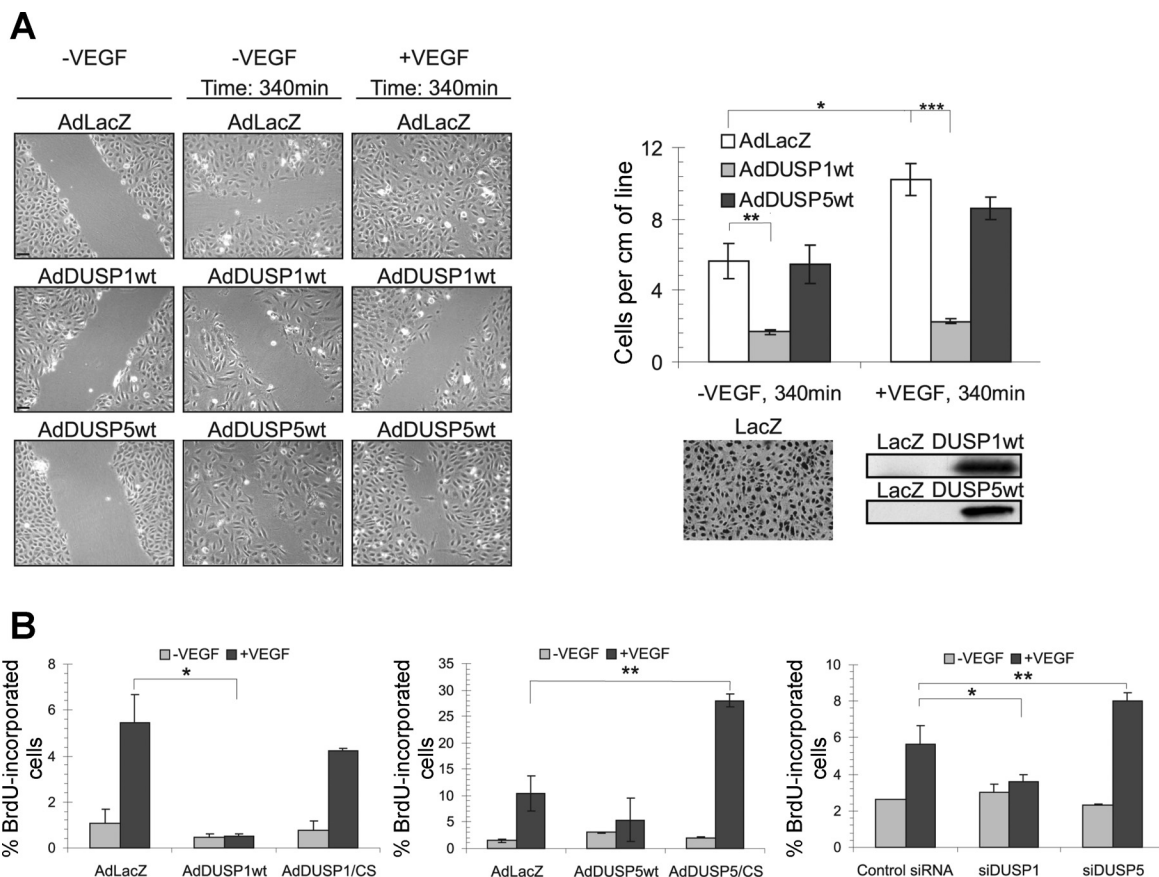


Fig. 7. Overexpression of DUSP1 and DUSP5 inhibits VEGF-induced migration and proliferation of endothelial cells. *A*: HUVECs were infected either with AdLacZ or AdDUSP1wt or AdDUSP5wt for 24 h. Subsequently, cell migration assay was performed according to MATERIALS AND METHODS. The graph shows images taken from noninduced cells at time points 0 and 340 min and from induced cells at the same time points, representing the number of the cells per centimeter of wound. Infection efficiency for AdLacZ, AdDUSP1wt, and AdDUSP5-expression levels are indicated below. The experiment shown is a representative one from three independent experiments.  $*P = 0.0038$ ,  $**P < 0.0001$ . Bar, 50  $\mu$ m. *B*: HUVECs were infected with AdLacZ, AdDUSP1wt, AdDUSP1/CS (*left*,  $*P = 0.0006$ ) or with AdLacZ, AdDUSP5wt, AdDUSP5/CS (*middle*,  $**P = 0.0002$ ) for 24 h or transfected with scrambled small interfering RNA (siRNA) or siDUSP1 or siDUSP5 for 72 h (*right*,  $*P = 0.0012$ ,  $**P = 0.0048$ ). Proliferation assay and indirect immunofluorescence was performed as indicated in MATERIALS AND METHODS. Graphs indicate percentage of BrdU-incorporated infected cells  $\pm$  SD derived from four independent experiments in the case of the *left* and *right* and six independent experiments in the case of the *middle*.

overstimulation of VEGF-induced EC proliferation, whereas DUSP1/CS did not exhibit such an effect (Fig. 7B, left and middle). Essentially similar results were obtained using siRNA-knockdown of DUSP1 and DUSP5 (Fig. 7B, right). The result is remarkably similar to the effect of DUSP1/CS and DUSP5/CS on VEGF-induced P-ERK1/2 levels (Fig. 5, C and D), strongly suggesting that DUSP5 is important in regulating EC proliferation. Thus DUSP5, by efficiently controlling dephosphorylation and anchoring of VEGF-induced P-ERK1/2 in the nucleus, plays a key role in controlling EC proliferation.

## DISCUSSION

Using microarray analysis and qRT-PCR validation, we have shown that VEGF dramatically activates transcription of the *DUSP1* and *DUSP5* genes. These DUSPs specifically dephosphorylate ERK1/2 and p38, pathways that are activated by VEGF in ECs and regulate key angiogenic responses such as migration and proliferation. Indeed, it has been recently shown that VEGF induces DUSP1/MKP-1 pointing also to the importance of DUSP1/MKP-1 in regulation of VEGF-stimulated EC migration (12). The present study adds DUSP5 to the VEGF-induced DUSPs in ECs. It appears, therefore, that VEGF induction of DUSP1/MKP-1 and DUSP5 might feedback on phosphorylated ERK1/2 and p38, thereby regulating the intensity and duration of these cascades in ECs. JNK is not activated by VEGF in HUVECs (27), a result that we have also observed in our HUVEC cultures (data not shown).

VEGF induces EC migration by activating p38 (13, 14, 27). Indeed, overexpression of DUSP1/MKP-1 in HUVECs completely abolished the VEGF-induced p38 phosphorylation and caused a dramatic inhibition of migration. Interestingly, the catalytically inactive form of DUSP1/MKP-1 did not lead to overstimulation of EC migration but rather exhibited no effect on migration of ECs (data not shown). Perhaps cells cannot be induced to migrate faster than a certain limit because of the need of actin polymerization and focal adhesion rearrangements. In the report of Kinney et al. (12), siRNA silencing of DUSP1/MKP-1 even decreased migration of ECs, overexpression of DUSP1/MKP-1 not being employed. It seems, therefore, that lack-of-function approaches of DUSP1/MKP-1 do not elicit the opposite effect of overexpression of this phosphatase, at least as far as migration of ECs is concerned. More work is apparently required on this issue. On the other hand, overexpression of DUSP5 did not have any effect on VEGF-induced phosphorylation of p38 or EC migration. These results strongly suggest that DUSP1/MKP-1 is the key phosphatase regulating the intensity and duration of VEGF-induced p38 phosphorylation and is in agreement with previous reports showing selectivity of DUSP1/MKP-1 toward P-p38 (26). Interestingly, DUSP1 gene transcription depends on p38 activation (20), a statement that is valid also in our cell system (supplemental Fig. 6).

In the present study, we conclusively show (using cell fractionation, immunohistochemistry, expression of eGFP-DUSP1, FLIM, and FCCS analysis) that DUSP1/MKP-1 is localized in both the cytoplasm and the nucleus of ECs, though DUSP1/MKP-1 is classified as an inducible nuclear DUSP (9). We additionally show that the cytoplasmic DUSP1/MKP-1 is in complex with unphosphorylated p38 with  $K_D^{\text{eff}}$  values of  $\sim 200$  nM, as suggested by our FLIM and FCCS experiments.

As p38-complexed DUSP1/MKP-1 is catalytically active (29), the pre-VEGF cytoplasmic concentration levels of DUSP1/MKP-1 may function as a threshold for VEGF-induced p38 phosphorylation requiring sufficient MKK3/6 activation by VEGF to overcome the dephosphorylating activity of DUSP1/MKP-1. Eventually, VEGF generates sufficient quantities of P-p38 that enters the nucleus of ECs, where it binds and activates its nuclear substrates, such as the transcription factor MEF2c and MK2a (18). Such binding is reflected in a strong increase of the  $K_D^{\text{eff}}$  (decrease in affinity) of the p38/DUSP1 interaction in FCCS, because the influxed P-p38-mCherry to the nucleus does not exhibit comobility with DUSP1-eGFP, as it is now bound to transcription factors or MK2a. Whereas transcription factors regulate transcription, the P-p38/P-MK2a heterodimer exits the nucleus (32) and phosphorylates cytoplasmic substrates such as HSP27 and LIMK1, thereby mediating VEGF-induced migration of ECs (27). As the levels of DUSP1/MKP-1 are increasing in the nucleus following VEGF induction, P-p38 will interact more frequently with DUSP1/MKP-1 eventually leading to dephosphorylation of P-p38, thereby ceasing activation of downstream transcription factors and p38-dependent transcriptional regulation. Also, formation of P-p38/P-MK2a complex will stop, thereby affecting migration of ECs. Moreover, the increasing levels of DUSP1/MKP-1 in the cytoplasm, following VEGF administration, will probably dephosphorylate cytoplasmic P-p38 ceasing activation of MK2a and its downstream substrates HSP27 and LIMK1, key mediators of VEGF-induced EC migration (13, 27). Thus both the nuclear and cytoplasmic DUSP1/MKP-1 could contribute to the regulation of VEGF-induced p-38 MAPK cascades (summarized in supplemental Fig. 7A), at least in ECs.

VEGF induces proliferation of ECs via activation of ERK1/2 (22). Upon phosphorylation, P-ERK1/2 enters the nucleus, where it is rapidly dephosphorylated (4, 33). Indeed, following VEGF induction, we have detected surprisingly low levels of P-ERK1/2 in the nucleus of ECs. It has been previously shown that the phosphatases responsible for nuclear inactivation of P-ERK1/2 are newly synthesized, show tyrosine or dual specificity, and interact with ERK1/2 via a KIM domain (33). On this basis, it has been suggested that the only phosphatases fulfilling these criteria are DUSP1/MKP-1 and DUSP4/MKP-2 (33). Here we show that VEGF induces DUSP1/MKP-1 and DUSP5, adding also the latter to the list of ERK1/2 inactivating phosphatases that fulfill the above criteria. The interaction between DUSP5 and ERK2 is significantly stronger than that between MKP-1/DUSP1 and ERK2 (19), also confirmed by our FCCS data in living ECs, suggesting that DUSP5 can contribute to the inactivation of ERK1/2. Indeed, inhibition of DUSP1/MKP-1 and DUSP5, by overexpressing the dominant-negative forms DUSP1/CS and DUSP5/CS (confirmed also by siRNA silencing) led to VEGF-induced proliferation that was  $\sim 80$  and  $170\%$  that of control, respectively, suggesting that DUSP5 contributes considerably to the dephosphorylation of P-ERK1/2 and the regulation of proliferation thereof. Interestingly, in the adipose tissue and skeletal muscles of *mkp-1<sup>-/-</sup>* mice both p38 and ERK1/2 were overactivated, whereas in the liver only overactivation of p38 was observed, ERK1/2 activity being slightly, but consistently reduced (35). Thus the relative involvement of DUSP1/MKP-1 in the dephosphorylation of ERK1/2 appears to be tissue or cell specific.

The importance of DUSP5 in regulation of VEGF-induced ERK1/2-dependent signaling is further intensified by the fact that DUSP5 is a nuclear anchor for ERK2 (19). Sequestration of ERK1/2 in a nuclear “anchoring and inactivating center,” away from the cytoplasmic MEK “activating center,” has been suggested to function as an efficient mechanism for signal termination (33). VEGF induction of DUSP5 appears to generate in ECs such an “inactivating and sequestering center.” We have shown here that overexpression of DUSP5 and DUSP5/CS sequesters ERK1/2 and P-ERK1/2 in the nucleus of ECs, respectively. The dephosphorylating and sequestering functions of DUSP5 on P-ERK1/2 is illustrated in the determination of the  $K_D^{\text{eff}}$  of the DUSP5-ERK2 complex by FCCS. After VEGF administration, the  $K_D^{\text{eff}}$  of the nuclear DUSP5-ERK2 interaction increases as a result of P-ERK2-mCherry influx, which interacts with target transcription factors exhibiting low comobility with DUSP5-eGFP. As VEGF increases the expression of DUSP5 in the nucleus, DUSP5 dephosphorylates and sequesters P-ERK1/2, thereby restoring the initial  $K_D^{\text{eff}}$  value of the DUSP5-eGFP/ERK2-mCherry association. Thus VEGF-induced upregulation of DUSP5 appears to contribute by dephosphorylating P-ERK1/2 and sequestering the dephosphorylated ERK1/2 in the nucleus of ECs, thereby terminating ERK1/2-dependent transcriptional regulation and proliferation, thereof (summarized in supplemental Fig. 7B).

In conclusion, VEGF strongly induces the transcription of two DUSP genes, *DUSP1* and *DUSP5*, in ECs. In distinction to the current assumption that DUSP1/MKP-1 is an inducible nuclear protein, DUSP1/MKP-1 is localized in both the nucleus and cytoplasm of ECs, whereas DUSP5 is a strictly nuclear protein. Our data suggest that DUSP1/MKP-1 dephosphorylates primarily VEGF-phosphorylated p38, thereby inhibiting EC migration, whereas DUSP5 and DUSP1/MKP-1 dephosphorylate VEGF-phosphorylated ERK1/2 inhibiting proliferation of ECs. Moreover, DUSP5 exhibits considerable nuclear anchoring activity on ERK1/2, thereby diminishing ERK1/2 export to the cytoplasm decreasing its further availability for activation. Thus induction of these phosphatases by VEGF serves as an autoregulatory circuit that controls activation of ERK1/2 and p38 cascades by the same growth factor, thereby regulating angiogenic responses of ECs, such a proliferation and migration.

#### ACKNOWLEDGMENTS

We thank the confocal laser microscope facility of the University of Ioannina for the use of the Leica TCS-SP scanning confocal microscope.

#### GRANTS

Part of this research was cofunded by the European Union in the framework of the program “Heraklitos” of the “Operational Program for Education and Initial Vocational Training” of the 3rd Community Support Framework of the Hellenic Ministry of Education, funded by 25% from national sources and by 75% from the European Social Fund (ESF). This study/research project received also financial support by the European Commission under the 6th Framework Programme (Contract No: LSHM-CT-2005-018725, PULMOTENSION).

#### DISCLOSURES

This publication reflects only the author(s)'s views and the European Community is in no way liable for any use that may be made of the information contained therein. No conflicts of interest are declared by the author(s).

#### REFERENCES

- Adams RH, Alitalo K. Molecular regulation of angiogenesis and lymphangiogenesis. *Nat Rev Mol Cell Biol* 8: 464–478, 2007.
- Bacia K, Kim SA, Schuille P. Fluorescence cross-correlation spectroscopy in living cells. *Nature Methods* 3: 83–89, 2006.
- Bagli E, Stefaniotou M, Morbidelli L, Ziche M, Psillas K, Murphy C, Fotsis T. Luteolin inhibits vascular endothelial growth factor-induced angiogenesis; inhibition of endothelial cell survival and proliferation by targeting phosphatidylinositol 3'-kinase activity. *Cancer Res* 64: 7936–7946, 2004.
- Costa M, Marchi M, Cardarelli F, Roy A, Beltram F, Maffei L, Ratto GM. Dynamic regulation of ERK2 nuclear translocation and mobility in living cells. *J Cell Sci* 119: 4952–4963, 2006.
- Dickinson RJ, Keyse SM. Diverse physiological functions for dual-specificity MAP kinase phosphatases. *J Cell Sci* 119: 4607–4615, 2006.
- Ferrara N, Gerber HP, LeCouter J. The biology of VEGF and its receptors. *Nature Med* 9: 669–676, 2003.
- Jaffe EA, Nachman RL, Becker CG, Minick CR. Culture of human endothelial cells derived from umbilical veins. Identification by morphologic and immunologic criteria. *J Clin Invest* 52: 2745–2756, 1973.
- Jeffrey KL, Camps M, Rommel C, Mackay CR. Targeting dual-specificity phosphatases: manipulating MAP kinase signalling and immune responses. *Nat Rev Drug Discov* 6: 391–403, 2007.
- Keyse SM. Dual-specificity MAP kinase phosphatases (MKPs) and cancer. *Cancer Met Rev* 27: 253–261, 2008.
- Keyse SM. Protein phosphatases and the regulation of mitogen-activated protein kinase signalling. *Current Opin Cell Biol* 12: 186–192, 2000.
- Keyse SM, Ginsburg M. Amino acid sequence similarity between CL100, a dual-specificity MAP kinase phosphatase and cdc25. *Trends Biochem Sci* 18: 377–378, 1993.
- Kinney CM, Chandrasekharan UM, Mavrikakis L, Dicorleto PE. VEGF and thrombin induce MKP-1 through distinct signaling pathways: role for MKP-1 in endothelial cell migration. *Am J Physiol Cell Physiol* 294: C241–C250, 2008.
- Kobayashi M, Nishita M, Mishima T, Ohashi K, Mizuno K. MAPKAPK-2-mediated LIM-kinase activation is critical for VEGF-induced actin remodeling and cell migration. *EMBO J* 25: 713–726, 2006.
- Lamalice L, Houle F, Jourdan G, Huot J. Phosphorylation of tyrosine 1214 on VEGFR2 is required for VEGF-induced activation of Cdc42 upstream of SAPK2/p38. *Oncogene* 23: 434–445, 2004.
- Lin YW, Yang JL. Cooperation of ERK and SCFskp2 for MKP-1 destruction provides a positive-feedback regulation of proliferating signaling. *J Biol Chem* 281: 915–926, 2006.
- Maciag T, Cerundolo J, Isley S, Kelley PR, Forand R. An endothelial cell growth factor from bovine hypothalamus: identification and partial characterization. *Proc Natl Acad Sci USA* 76: 5674–5678, 1979.
- Maeder CI, Hink MA, Kinkhabwala A, Mayr R, Bastiaens PI, Knop M. Spatial regulation of Fus3 MAP kinase activity through a reaction-diffusion mechanism in yeast pheromone signalling. *Nat Cell Biol* 9: 1319–1326, 2007.
- Maiti D, Xu Z, Duh EJ. Vascular endothelial growth factor induces MEF2C and MEF2-dependent activity in endothelial cells. *Invest Ophthalmol Visual Sci* 49: 3640–3648, 2008.
- Mandl M, Slack DN, Keyse SM. Specific inactivation and nuclear anchoring of extracellular signal-regulated kinase 2 by the inducible dual-specificity protein phosphatase DUSP5. *Mol Cell Biol* 25: 1830–1845, 2005.
- McMullen ME, Bryant PW, Glembotski CC, Vincent PA, Pumiglia KM. Activation of p38 has opposing effects on the proliferation and migration of endothelial cells. *J Biol Chem* 280: 20995–21003, 2005.
- Meadows KN, Bryant P, Pumiglia K. Vascular endothelial growth factor induction of the angiogenic phenotype requires Ras activation. *J Biol Chem* 276: 49289–49298, 2001.
- Olsson AK, Dimberg A, Kreuger J, and Claesson-Welsh L. VEGF receptor signalling in control of vascular function. *Nat Rev Mol Cell Biol* 7: 359–371, 2006.
- Owens DM, Keyse SM. Differential regulation of MAP kinase signalling by dual-specificity protein phosphatases. *Oncogene* 26: 3203–3213, 2007.
- Panopoulou E, Murphy C, Rasmussen H, Bagli E, Rofstad EK, Fotsis T. Activin A suppresses neuroblastoma xenograft tumor growth via antimitotic and antiangiogenic mechanisms. *Cancer Res* 65: 1877–1886, 2005.
- Pearson G, Robinson F, Beers Gibson T, Xu BE, Karandikar M, Berman K, Cobb MH. Mitogen-activated protein (MAP) kinase pathways: regulation and physiological functions. *Endocr Rev* 22: 153–183, 2001.
- Pratt PF, Bokemeyer D, Foschi M, Sorokin A, Dunn MJ. Alterations in subcellular localization of p38 MAPK potentiates endothelin-stimulated COX-2 expression in glomerular mesangial cells. *J Biol Chem* 278: 51928–51936, 2003.

27. **Rousseau S, Houle F, Landry J, Huot J.** p38 MAP kinase activation by vascular endothelial growth factor mediates actin reorganization and cell migration in human endothelial cells. *Oncogene* 15: 2169–2177, 1997.
28. **Sakurai Y, Ohgimoto K, Kataoka Y, Yoshida N, Shibuya M.** Essential role of Flk-1 (VEGF receptor 2) tyrosine residue 1173 in vasculogenesis in mice. *Proc Natl Acad Sci USA* 102: 1076–1081, 2005.
29. **Slack DN, Seternes OM, Gabrielsen M, Keyse SM.** Distinct binding determinants for ERK2/p38alpha and JNK map kinases mediate catalytic activation and substrate selectivity of map kinase phosphatase-1. *J Biol Chem* 276: 16491–16500, 2001.
30. **Takahashi T, Yamaguchi S, Chida K, Shibuya M.** A single autophosphorylation site on KDR/Flk-1 is essential for VEGF-A-dependent activation of PLC-gamma and DNA synthesis in vascular endothelial cells. *EMBO J* 20: 2768–2778, 2001.
31. **Tanoue T, Nishida E.** Molecular recognitions in the MAP kinase cascades. *Cell Signal* 15: 455–462, 2003.
32. **ter Haar E, Prabhakar P, Liu X, Lepre C.** Crystal structure of the p38 alpha-MAPKAP kinase 2 heterodimer. *J Biol Chem* 282: 9733–9739, 2007.
33. **Volmat V, Camps M, Arkinstall S, Pouyssegur J, Lenormand P.** The nucleus, a site for signal termination by sequestration and inactivation of p42/p44 MAP kinases. *J Cell Sci* 114: 3433–3443, 2001.
34. **Wouters FS, Vermeer PJ, Bastiaens PI.** Imaging biochemistry inside cells. *Trends Cell Biol* 11: 203–211, 2001.
35. **Wu JJ, Roth RJ, Anderson EJ, Hong EG, Lee MK, Choi CS, Neuffer PD, Shulman GI, Kim JK, Bennett AM.** Mice lacking MAP kinase phosphatase-1 have enhanced MAP kinase activity and resistance to diet-induced obesity. *Cell Metab* 4: 61–73, 2006.

